

A Robust Technique to Characterize the Palmprint using Radon Transform and Delaunay Triangulation

Amel Bouchemha

Department of Electrical Engineering
Faculty of Engineering Sciences
University of Tebessa, 12000, Algeria

Amine Nait-Ali

Université Paris-Est Créteil
Laboratory of Image, Signal
and Intelligent System (LISSi,
E.A 3956), 61 Avenue du général
De Gaulle, 94010, Créteil, France

Nourredine Doghmane

Department of Electronics
faculty of Engineering Sciences
University of Annaba, 23000, Algeria

ABSTRACT

For the purpose of biometric applications, we explore in this paper a new robust approach to characterizing palmprint features. Instead of processing the acquired image in the spatial domain, the proposed technique extracts palmprint features using Radon transform and a geometric Delaunay triangulation jointly. In such a process, Radon transform enables the extraction of directional characteristics from the palm of the hand. Afterwards, the most significant information is structured using Delaunay triangulation, thus providing a specific palmprint signature. In order to compare the uniqueness as well as the stability of the palmprint signature, Hausdorff distance has been used as a criterion of similarity. As will be shown in this paper, the palmprint signature is very robust even when considering a low Signal-to-Noise Ratio (SNR). Promising results are obtained from a local database containing 200 palmprint images. This technique is mainly appropriate for authentication applications.

Keywords

Biometric, Palmprint, Radon transform, Delaunay triangulation, Hausdorff distance, Authentication

1. INTRODUCTION

Biometrics is a field of science and technology whose goal is the identification or verification of individual identities using their physiological and behavioral characteristics. Certain forms of measurement related to the physiology of the individuals such as fingerprints and palmprints are commonly considered to be the most reliable techniques when dealing with individual automatic identification or verification.

Within this context, the palmprint, in comparison to other modalities, has several advantages therefore making its use easy and practical. For instance, only low-resolution images are required and low cost capturing devices can be used. Moreover, one can easily extract several features required for both identification and verification purposes such as principal lines, wrinkles, ridges, minutiae points, singular points, texture, etc. Texture and palm lines are the most clearly observable in low resolution. For this reason, they are extensively employed in verification applications. From the existing literature, several methods have been proposed to date. Primarily, these methods are based upon morphological characteristics [1, 21]. For example, Zhang et al. [10] use a Gabor filter to extract what has been called "Palm code" [10]. Chen and Xie [15] use a dual tree complex wavelet to extract the textural energy of the palmprint. Lie and You have proposed a texture-based retrieval scheme palmprint using a layered search [22]. Zhang and Zhang use a wavelet template over-directional context modeling and expansion

to extract principal lines as features [16]. Han et al. propose Sobel and morphological operations to extract the lines [4]. In [8], the principal lines are extracted using a Modified finite Radon transform to extract the principal lines. Appearance based approaches have also been reported in the literature. They provide interesting results but they may be sensitive to illumination, contrast, and position changes. Lu et al [14] and Wu et al, [26] have proposed two methods based on Principal Component Analysis (PCA) and linear discriminant analysis (LDA), respectively. Connie et al. have proposed several ACP / LDA / ICA-based approaches. The palmprint images are analyzed in a multi-resolution and a multi-frequency representation using wavelet transform [19].

In our work, a new approach to characterizing the palmprint is proposed. The corresponding image is processed in Radon Domain which has the specificity (1) to transform perfect lines into points, (2) to be robust regarding noise. Consequently, even when the hand lines are not perfectly rectilinear, RT allows a local concentration of the energy for which one can encode their positions. Afterwards, main feature points are connected using Delaunay triangulation for the purpose of defining a unique topological structure for each individual.

The rest of the paper is organized as follows: Section 2 discusses the proposed approach which includes the extraction of Region-Of-Interest (ROI) and the principal lines. Afterwards, we briefly describe the Radon Transform, the extraction of features. We then develop the principal of Delaunay triangulation in order to extract a signature. In Section 3 we provide a criterion of comparison. In Section 4 we report on some experimental results where the robustness of the proposed technique is evaluated. Finally, our conclusions are presented in Section 5.

2. PROPOSED APPROACH

In this section we present the different steps required for characterizing the palmprint. For this purpose, three sub-sections are presented, namely: ROI extraction, palm lines extraction and finally the processing step in the Radon domain. Figure 1, shows the block diagram of the proposed algorithm.

In our approach, the maximum values of Radon coefficients will be used to characterize the specific primitives, such as straight lines or arcs of conics. Due to the inherent properties of Radon transform, we deem it a useful tool for the capture of directional features of images. Before the features extraction, it is first necessary to obtain a sub-image from the captured palm. Once the region of interest (ROI) has been extracted from the input image, a line-detector is applied to extract the principal lines.

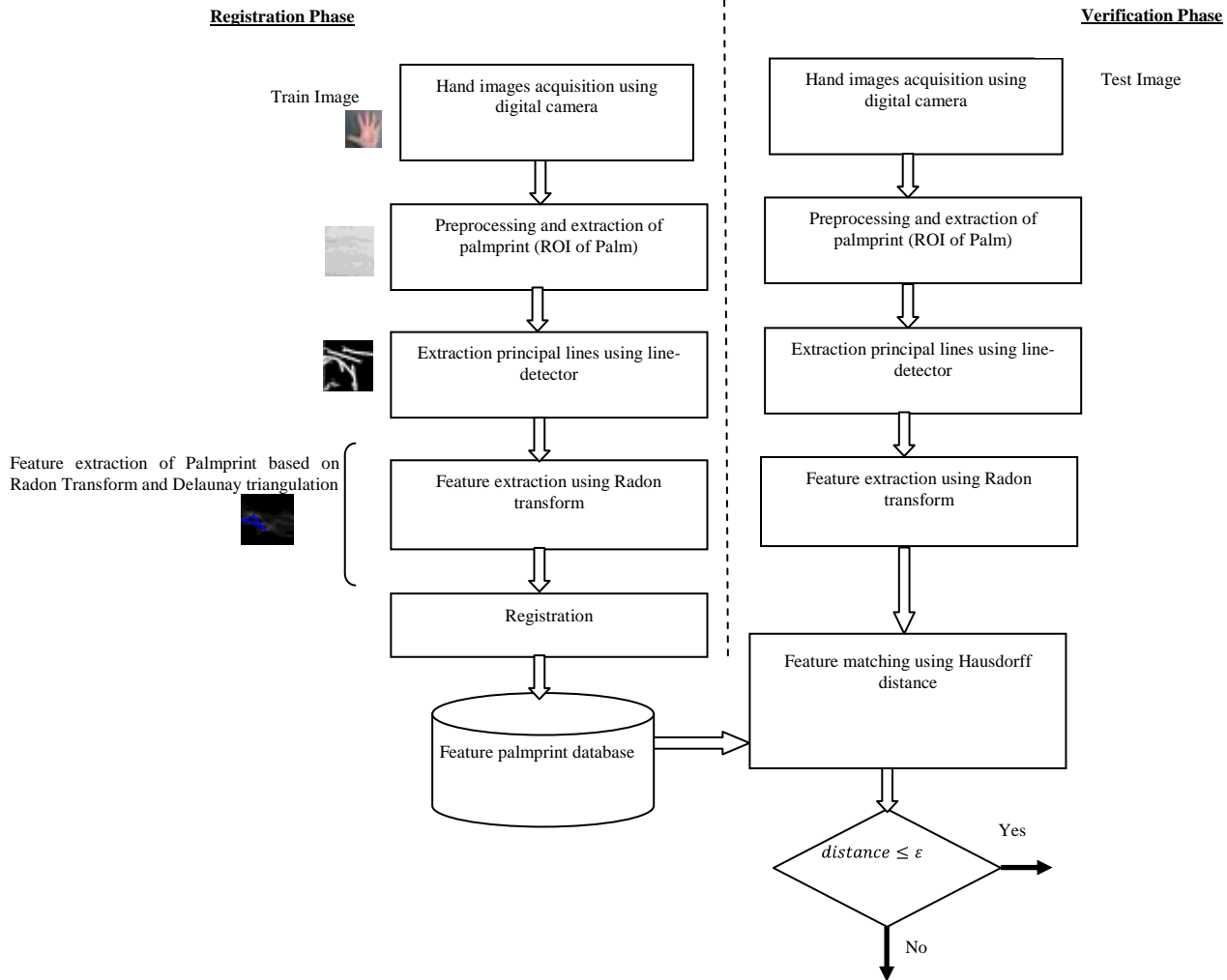


Figure 1 Block diagram of the proposed approach.

2.1 Extraction of the palmprint ROI

To extract the region of interest (ROI), we must do a pre-processing of the hand images. The image pre-processing stage involves hand image segmentation; key point determination and finally extraction of the ROI (see Figure 2). Based on the existing literature, several segmentation methods can be employed. These include: histogram based, clustering gray level based, entropy based, spatial coherence and adaptation local based methods. To extract a ROI from a hand image, two approaches can be used. The first approach extracts a square region [12, 13, 19, 21] whereas the second performs a circular region on the hand image.

In this work, the ROI is extracted using the following steps:

Step 1: a simple thresholding is used to separate the hand region from the background. In this case a threshold γ is required to convert the gray image into a binary map (see Figure 2.d).

Step 2: a neighborhood border tracing algorithm is used to obtain the contour of hand shape (see Figure 2.e)

Step 3: a valley detection algorithm is used to detect the valleys of the fingers (see Figure 2.f).

Step 4: the obtained valleys serve as basic points in order to locate the region of the palmprint (see Figure 2.f). In this case it is necessary to set up a coordinate system that is invariant to the rotation and translation of the palm.

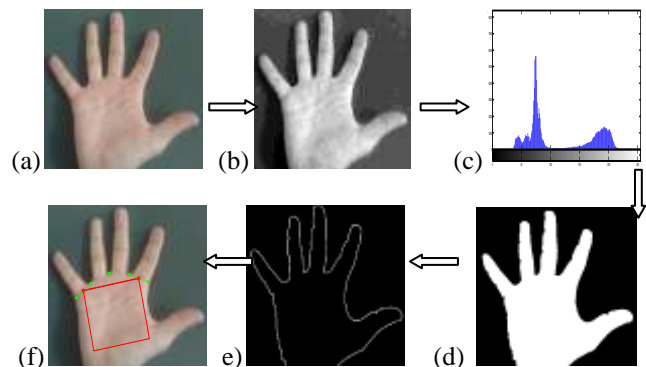


Figure 2 Extract of ROI : (a) original image ; (b) Gray level image ; (c) histogram of image ; (d) Binarized image ; (e) Contour image of (d) ; (f) Extract ROI

2.2 Line extraction

Both the location and the form of principal lines (such as *heart line*, *head line* and *life line*) in a palmprint are considered as important characteristics for the identification of individuals because of their stability and uniqueness [12]. This step requires the application of an average mask, a line detection mask, and finally thinning lines.

2.3 Characterization of the palm lines in Radon domain

2.3.1. Radon Transform

Generally speaking, Radon transform decomposes a function in terms of its integral projections [9, 17, 18, 23-25, 27]. Let $f(x, y)$ be the ROI of palmprint which contains the principal lines. The Radon transform $R_f(\beta, \theta)$ of $f(x, y)$ is a set of projection along the lines according to different angles θ . Thus $R_f(\beta, \theta)$ is defined as:

$$R_f(\beta, \theta) = \int_{-\infty}^{+\infty} \int_{-\infty}^{+\infty} f(x, y) \delta(x \cos(\theta) + y \sin(\theta) - \beta) dx dy \quad (1)$$

where $\theta \in [0, \pi]$ and $\beta \in [-\infty, +\infty]$, $\delta(\cdot)$ represents the Dirac function defined by: $\int_{-\infty}^{+\infty} \delta(t) dt = 1$ and $\delta(t) = 0$ if $t \neq 0$. If we consider a straight line expressed by:

$$L(x, y) = \delta(\beta^* - x \cos \theta^* - y \sin \theta^*) \quad (2)$$

The Radon transform of the function $L(x, y)$ is:

$$R_L(\beta, \theta) = 0 ; \quad \beta \neq \beta^* \text{ or } \theta \neq \theta^*$$

$$R_L(\beta, \theta) = \int \delta(0); \quad \beta = \beta^* \text{ and } \theta = \theta^*$$

The Radon transform of a line with the parameters β^*, θ^* is in the space of Radon, a Dirac located on $[\beta^*, \theta^*]$ (see Figure 3). Thus, one can estimate the parameters of a line from the Radon transform of an image.

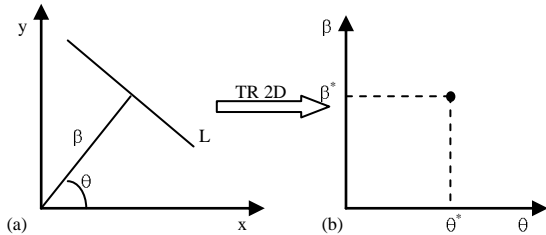


Figure 3 Representation of a straight line; (a) in the spatial domain and (b) in the Radon domain.

Radon transform is interesting when considering various properties related to the translation, rotation and scaling as expressed by the following equations:

-Translation

$$R(\beta, \theta) \{f(x - x_0, y - y_0)\} = R_f(\beta - \beta_0, \theta) \quad (3)$$

-Rotation

$$R(\beta, \theta) \{f(x \cdot \cos \varphi + y \cdot \sin \varphi, -x \cdot \cos \varphi + y \cdot \sin \varphi)\} = R_f(\beta, \theta + \varphi) \quad (4)$$

-Scaling

$$R(\beta, \theta) \left\{ f \left(\frac{x}{\lambda}, \frac{y}{\lambda} \right) \right\} = \lambda \cdot R_f \left(\frac{\beta}{\lambda}, \theta \right) \quad (5)$$

Here $\beta_0 = x_0 \cos \theta + y_0 \sin \theta$, λ : the scaling factor and φ is the rotation angle.

From these equations, a translation of $f(x, y)$ results in a shift of $R(\beta, \theta)$ by a distance equal to the projection of the translation vector (x_0, y_0) on the line $\beta = x \cos \theta + y \sin \theta$.

A rotation of $f(x, y)$ by an angle φ leads to a translation of $R(\beta, \theta)$ along θ . A scaling of $f(x, y)$ results in a scaling in the β coordinate, as well as an intensity scaling of $R(\beta, \theta)$.

To characterize the ROI image $f(x, y)$ of a palmprint, it is particularly interesting to consider the case containing only the principal lines of the palmprint without outliers. Let:

$$f_L(x, y) = \begin{cases} 1 & \text{si } (x, y) \in L \\ 0 & \text{elsewhere} \end{cases} \quad (6)$$

where L is each of the principal lines. Several key features that are compatible with human visual perception can be extracted in the domain of Radon transform. We note that the projection lines at different angles contain crucial information that helps to characterize the structure of the palmprint. The geometric forms such as straight lines or curves can be presented explicitly by the Radon transform which concentrates energies from the image into a few high-valued coefficients in the transformed domain.

2.3.2. Feature extraction

From Radon transform, only the coefficients greater than a threshold are considered. First, we start by extracting the maximum value of Radon coefficients along each projection θ_i . The following equation optimizes the Radon transform:

$$S_R(\theta_i) = \max_{\beta} \{ |R_{f_L}(\beta, \theta_i)| \} \quad (7)$$

where $\theta_i \in [0, \pi]$. Then, we use an appropriate thresholding for each class of palmprint images as follows:

$$M_{\text{threshold}}(\beta, \theta_i) = S_R(\beta, \theta_i) > \text{Threshold} \quad (8)$$

where **Threshold** is calculated based on the maximum and the average of Radon coefficients. To adapt the threshold for each specific class of palmprint, we introduced an adaptive empirical factor α . The following equation gives the expression of the appropriate threshold:

$$\text{Threshold} = \mu + \frac{(\text{max} - \mu)}{\alpha} \quad (9)$$

α : adaptive factor, μ : mean of Radon coefficients, **max**: the maximum of the Radon coefficients along each projection.

Once the coefficients of Radon transform are extracted, thresholded and binarized, the representation of palmprint becomes a set of distinct objects. In order to measure the similarity between the different structures, we will identify them by their geometric attributes. Some simple geometric features can be used to describe the signature of the palmprint. In our work, we extract the centroid of each region (high concentration of energy) and eliminate others which are considered as outliers.

2.3.3. Feature modeling using Delaunay Triangulation

We have seen previously how to extract characteristics from the Radon domain. In this section, the dominant points are connected to each other by means of Delaunay triangulation in order to produce a unique [15, 18, 24, 27], where the processing is achieved on $f_L(x, y)$ which represents the Binary ROI image geometrical signature corresponding to the analyzed palmprint.

Within such a context, let S denote a set of main points $s_1, s_2, s_3, \dots, s_n$, obtained after the thresholding and the binarization processes of the Radon transform image. Delaunay triangulation of S is computed by first calculating the Voronoi diagram. The Voronoi diagram decomposes the 2D space into polygonal region around each point s_i such that all points of the region s_i are closer to S_i than any other point of S . Given the Voronoi diagram, the Delaunay triangulation can be formed by connecting the centers of every pair of neighboring Voronoi regions. In addition to the uniqueness of the Delaunay triangulation, another property of this triangulation is that it maximizes the smallest angle of all triangles. Consequently, one can obtain a regular triangulation [2, 20]. The basic idea is to establish a stable structure of characteristics. One has to point out that the geometrical signature is not sensitive to rotations, which means that the main features are unmodified for a given class.

After binarization of the matrix Radon transform, we extract the centroids of objects in the image and eliminate the outliers (points with small value). Let C the set of all centroids which form the signature of the palmprint:

$$C = [c_1, c_2, c_3, \dots, c_n] \quad (10)$$

where $c_n = (x_n, y_n)$ represents the coordinates of the centroid of the object in image.

Once the centroids are extracted in the Radon domain, we use the Delaunay triangulation where the vertices are these centroids, each palmprint is then represented by a particular connected graph with each node constituting a point of Radon transform and each segment connecting two centroids. To compare two structures obtained by Delaunay triangulation of the palmprint, in our approach we used the Hausdorff distance as a metric of measure similarity.

3. SIMILARITY MEASUREMENT

We need to compare the input image with the training images in the database to determine which training image is most similar to the input image. To show the matching performance of the proposed approach, we have used the Hausdorff measure. The geometrics-based image matching approach is regarded as being more robust against the intensity-based image matching approach. Hausdorff distance has been recognized as providing an effective way for image matching. The Hausdorff distance provides a measure between two point sets. Unlike most of shape recognition techniques which require a one-to-one correspondence between the template and the testing data, the Hausdorff distance can be found without explicit point correspondence [3, 5-7, 11].

Given two finite points sets $C = \{c_1, c_2, \dots, c_p\}$ and $C' = \{c'_1, c'_2, \dots, c'_p\}$. Hausdorff distance is the maximum distance of a set to the nearest point in the other set [3, 5-7, 11]. Mathematically, Hausdorff distance from set C to set C' is a maximum function defined as:

$$H(C, C') = \max(h(C, C'), h(C', C)) \quad (11)$$

Where $h(C, C') = \max_{c \in C} \{\min_{c' \in C'} \{d(c, c')\}\}$, where c, c' the centroids are extracted from Radon coefficients and $d(c, c')$ can

be any metric between these points. For purposes of simplicity, $d(c, c')$ is considered as the Euclidian distance between c and c' . Therefore, one can measure the tolerance of the Delaunay triangulation of two sets of points C and C' based on the measurement of the distance of Hausdorff. Let $DT(C)$ and $DT(C')$ the Delaunay triangulation of the sets C and C' . The tolerance is defined as the supremum of all $\varepsilon \geq 0$ such that if each point c_i is moved arbitrarily the structure $DT(C)$ does not change. It is defined as follows:

$$tol(DT(C)) = \text{Sup} \left\{ \begin{array}{l} \varepsilon \geq 0 \mid DT(C) \sim DT(C') \text{ for all } C' \\ \text{such that } h(C, C') < \varepsilon \end{array} \right\} \quad (12)$$

where $DT(C) \sim DT(C')$ means that c_i and c_j are Delaunay neighbors in $DT(C)$ if and only if the corresponding points c'_i and c'_j are Delaunay neighbors in $DT(C')$.

4. RESULTS AND DISCUSSION

To evaluate the performance of the proposed scheme, a local specific contactless palmprint database has been used. This database contains 200 images collected from 20 individuals. These images were acquired by a digital camera having a resolution of 1280 x 960 pixels and located at a distance between 20 and 50 cm from the palm. Figure 4 shows the digital device used in our laboratory. Originally, the collected images were 300x300. The central parts of each image are extracted at a size of 128x128.

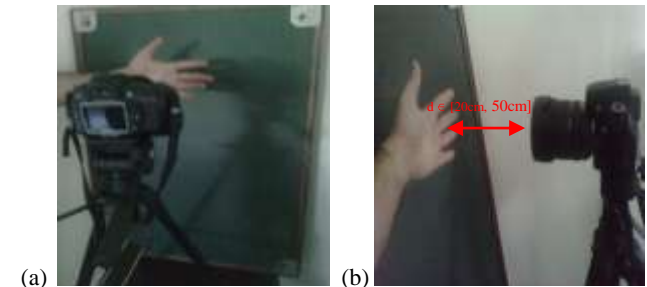


Figure 4 Acquisition system of hand images (a) acquisition of typical image; (b) the distance used in the acquisition

4.1 Extract principal lines and Radon features of ROI

Once the ROI was extracted from the hand image, we applied a line-detector to find the principal lines of palmprint. Figures 5.a and 5.b show the palmprint of several acquisitions of hand images and principal lines following the normalization of each acquisition. After this, the image of palmprint is projected in Radon domain. Note that in the space of Radon transform, some of the coefficients are more significant than others (see Figure 5.c).

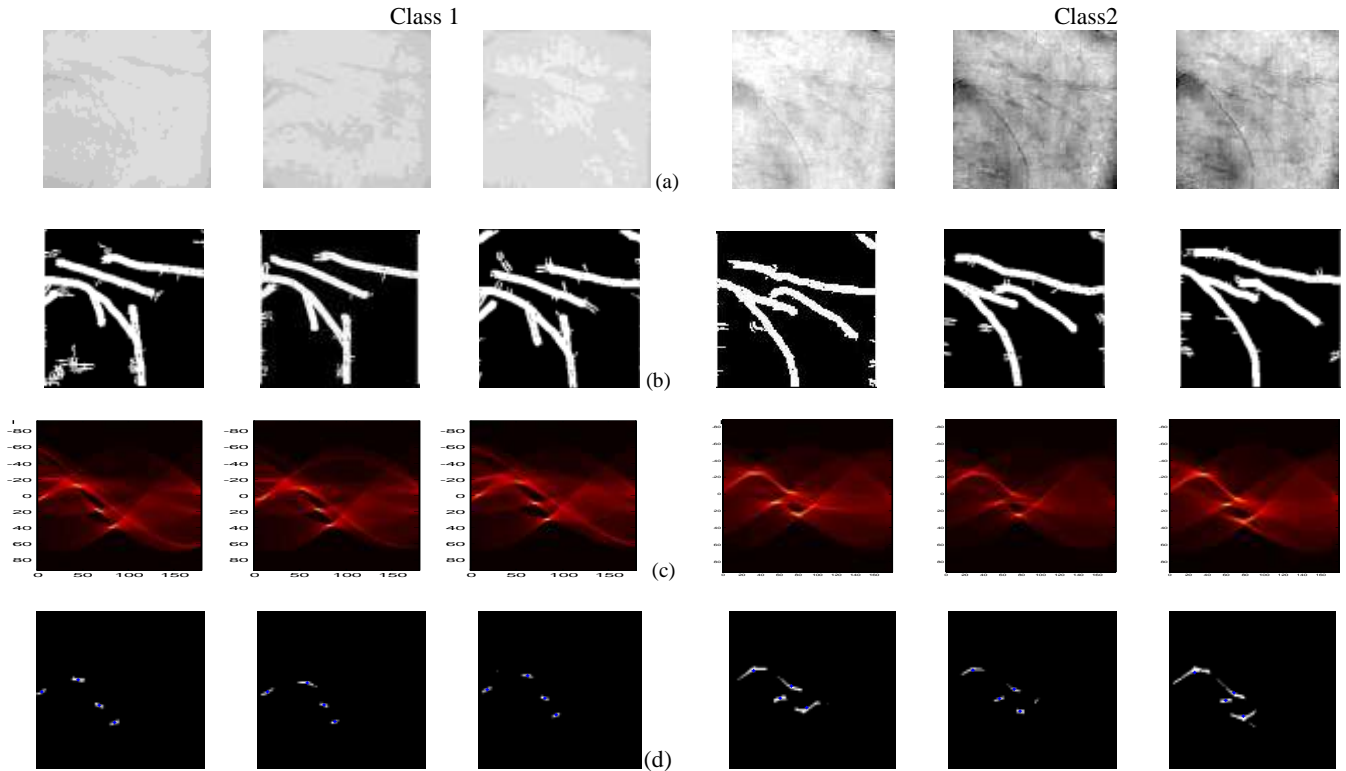


Figure 5 Radon transform of the principal lines of ROI for 2 classes of palmprint with several acquisitions; (a) Palmprint images; (b) Principal lines of palmprint; (c) Radon transform of ROI; (d) Centroids extraction using the thresholding and binarized Radon coefficients

By representing the histogram of Radon coefficients according to several projections (see Figure 6), we note that there is a maximum for each projection angle which corresponds to a high concentration of energy.

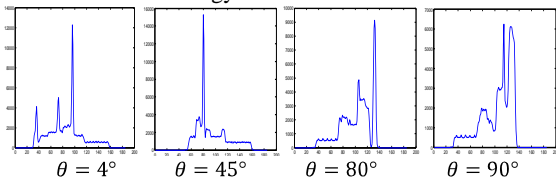


Figure 6 Histogram of Radon coefficients for several projections ($\theta = 4, 45, 80$ and 90°)

To keep only the maximum coefficient of Radon transform for each projection, we applied an adaptive thresholding to each class of palmprint images. As a result, we obtained a simple representation as a set of distinct objects that can be characterized by a set of features. In our approach, we have considered the centroids for each shape (object) (see Figure 5.d). We carried out the simulation on several different classes with several acquisitions. Consequently, we were able to notice visually that for an appropriate threshold and for each class of image palmprint, the signature obtained by the Delaunay triangulation is stable for the various acquisitions. It is specific to each palmprint (see Figure 7).

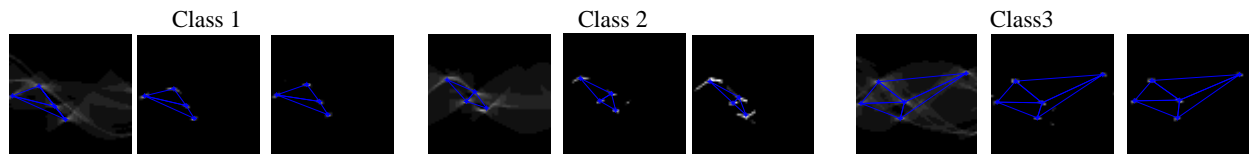


Figure 7 Representation of the Delaunay triangulation for the several classes of palmprint with several acquisitions.

The rotation of palmprint images at an angle causes a shift of the Radon transform of a quantity proportional to the rotation. The

characterization using centroids and Delaunay triangulation, remains stable (see Figure 8).

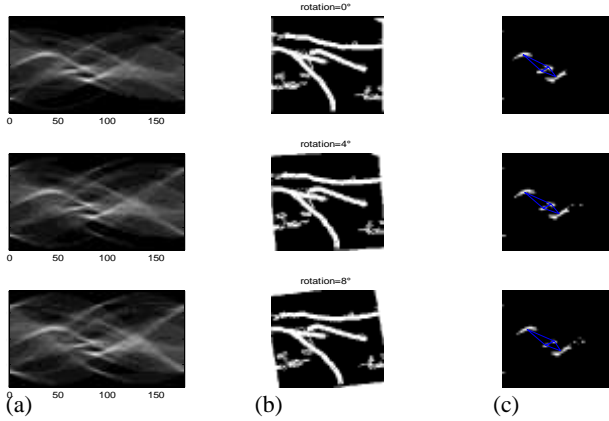


Figure 8 Rotation-invariant of Radon; (a) Coefficients of Radon transform; (b) Rotation of ROI for $\theta = 4^\circ$ and 8° ; (c) Extraction features and Delaunay triangulation

4.2 Measure of similarity of Delaunay triangulation

In order to objectively measure the similarity between two signatures, Hausdorff distance has been calculated using the acquired signature and a reference one stored in a database. The lower the distance, the higher the similarity with which to identify an individual. Table 1 provides the results obtained from several palmprints showing that each signature is stable and unique. Ideally, one can consider that an acquired signature matches with

a given reference if Hausdorff distance is zero. In practice, this distance should be lower than a tolerance ϵ .

4.3 Robustness of structure to additive noise

To evaluate the robustness of this method to additive noise, a Gaussian noise is added to the acquired palmprint image with principal lines. For this purpose, various SNRs (Signal to Noise Ratios (dB)) have been considered. Figure 9, shows the robustness of the Radon transform to noise and the stability of the Delaunay triangulation (SNR=11.20 dB, SNR=7.27 dB and SNR=4.75 dB).

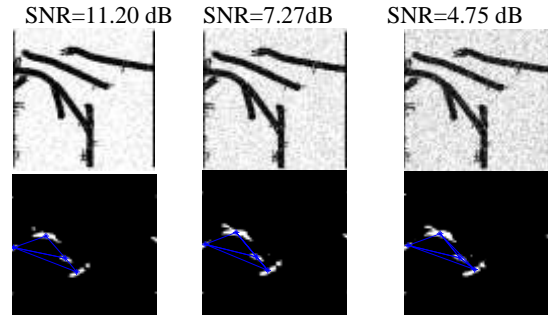


Figure 9 Delaunay Triangulation of noised image of principal lines with several SNR

Table 1. Measurement of similarity using the Hausdorff distance for different class of palmprint with several acquisitions

	0	7.45	10.33	8.67	11.18	38.51	42.97	35.59	33.13	41.79	39.69	38.99
	7.45	0	13.19	16.30	12.15	33.16	38.13	29.96	32.63	37.76	37.04	32.78
	10.33	13.19	0	13.37	13.93	35.25	39.33	32.59	31.57	40.75	38.65	36.55
	8.67	16.30	13.37	0	10.41	31.42	34.90	27.70	29.99	36.44	35.63	31.12
	11.18	12.15	13.93	10.41	0	35.29	39.79	30.86	34.28	37.19	35.73	32.42
	38.51	33.16	35.25	31.42	35.29	0	14.01	5.93	7.89	22.25	21.08	14.54
	42.97	38.13	39.33	34.90	39.79	14.01	0	10.08	13.74	22.84	22.15	16.07
	35.59	29.96	32.59	27.70	30.86	5.93	10.08	0	8.49	22.57	21.33	14.74
	33.13	32.63	31.57	29.99	34.28	7.89	13.74	8.49	0	28.33	27.14	20.88
	41.79	37.76	40.75	36.44	37.19	22.25	22.84	22.57	28.33	0	3.07	16.29
	39.69	37.04	38.65	35.63	35.73	21.08	22.15	21.33	27.14	3.07	0	16.8
	38.99	32.78	36.55	31.12	32.42	14.54	16.07	14.74	20.88	16.29	16.78	0

Consequently, one can say that the characterization of the palmprint using the Radon transform and the Delaunay triangulation is stable and unique for the same palmprint despite the disruption caused by noise. Table 2 gives the Hausdorff distance between the Delaunay triangulation of image and noised image. We see that it remains low, which confirms once again the robustness of our approach to additive noise. We have also simulated disruptions other than additive Gaussian noise and the results are very promising

Table 2. Measurement similarity of noisy image with several SNR (dB) using Hausdorff distance

Noised Image					
Variance	0.02	0.03	0.05	0.09	0.1
SNR (dB)	11.20	9.50	7.27	4.75	4.28
Hausdorff distance	1.78	1.83	1.95	4.08	4.98

5. CONCLUSION

In this work we have presented a new approach to characterizing the palmprint of an individual using both Radon transform and Delaunay triangulation. This approach extracts invariant features from Radon projection of an image obtained after a pre-processing phase in which the principal lines are extracted using an entropic line-detector. Consequently, experimental results show that this approach allows a high stability and provides a good robustness to noise. Using several classes of palmprints, a set of features involving statistical and visual attributes were extracted. However, due to the fact that the number of centroids of Radon transform pattern is relatively small compared to those for minutiae, analysis based on geometrical information is preferred to statistical features. Moreover, since the palmprint pattern is represented as a set of two-dimensional points, matching a pair of such patterns can be achieved easily by measuring the Hausdorff distance between two centroid sets. Based on the obtained results promising performances have been obtained. For future work, the proposed technique can be improved by merging each signature with other useful information such as hand texture.

6. REFERENCES

[1] A. Kumar, D. Zhang, “Personal authentication using multiple palmprint representation”, *Pattern Recognition*, vol. 38, 2005, 1695–1704

[2] A. Kumar, K. V. Prathysha, “Personal Authentication using hand vein triangulation”, *IEEE Transactions on Image Processing*, vol. 18, 2009, 2127–2136.

[3] C-B. Yu, H-F. Qin, Y-Z. Cui and XQ. Hu, “Finger-Vein Image Recognition Combining Modified Hausdorff Distance with Minutiae Feature Matching”, *Interdiscip Sci Comput Life Sci*, vol. 1, 2009, 280–289.

[4] C-C Hana, H.L Chengb, C.L Linb and K.C. Fanb, “Personal authentication using palm-print features”, *Pattern Recognition*, vol. 36, 2003, 371 – 381

[5] C-H.T. Yanga, S-H. Lai and L-W. Chang, “Hybrid image matching combining Hausdorff distance with normalized gradient matching”, *Pattern Recognition*, vol. 40, 2007, 1173 – 1181.

[6] C. Zhao, W. Shi and Y. Deng, “A new Hausdorff distance for image matching”, *Pattern Recognition Letters*, vol. 26, 2005, 581–586.

[7] D.P. Huttenlocher, G.A. Klanderman and W.J. Rucklidge, “Comparing images using the Hausdorff distance”, *IEEE Trans Pattern Anal Mach Intel*, vol 15, n°9, 1993, 850–863.

[8] D. S Huang, W. Jia and D. Zhang, “Palmprint verification on principal lines”, *Pattern Recognition*, vol. 41, 2008, 1316-1328.

[9] D.V. Jadhav, R. Holambe, “Feature extraction using Radon and wavelet transforms with application to face recognition”, *Neuro computing*, vol.72, 2009, 1951–1959.

[10] D. Zhang, A. Kong, J. You and M. Wong, “Online palmprint identification”, *IEEE Trans. Pattern Anal. Mach. Intel*, vol. 25, n°9, 2003, 1041–1050.

[11] E.P. Vivek, N. Sudha, “Gray Hausdorff distance measure for comparing face images”, *IEEE Transactions on Information, Forensics and Security*, vol. 1, 2006, 342–349.

[12] F. Li, M. K.H. Leung and C.S. Chian, “Making Palm Print Matching Mobile”, (*IJCSIS*) *Inter. Journal of Computer Science and Information Security*, vol.6, n° 2, 2009.

[13] G. Kah Ong Michael, T. Connie and A. Beng Jin Teoh, “Touch-less palm print biometrics: Novel design and implementation”, *Image and Vision Computing*, vol. 26, 2008, 1551–1560.

[14] G. Lu, D. Zhang and K. Wang, “Palmprint recognition using eigenpalms features”, *Pattern Recognition. Letters*, vol. 24, 2003, 1463–1467.

[15] G.Y. Chen, W.F. Xie, “Pattern recognition with SVM and dual-tree complex wavelets”, *Image Vis. Computing*, vol. 6, 2007, 960–966.

[16] L. Zhang, D. Zhang, “Characterization of palmprints by wavelet signatures via directional context modeling”, *IEEE trans. Syst. Man, and cybernetics, Part B: Cybernetics*, vol. 34, n°3, 2004, 1335-1347.

[17] Q. Zhang, I. Couloiger, ”Accurate Centerline Detection and Line width estimation of thick Lines Using the Radon Transform”, *IEEE Trans. On Image processing*, vol. 16, n° 2, 2007, 310-316.

[18] S. Tabbone, L. Wending and J.P Salmon, “A new shape descriptor defined on the Radon transform”, in *Computer Vision and Image Understanding*, vol.102, 2006, 42-51.

[19] T. Connie, A.T. Beng Jin, M. Goh Kah Ong and D. Ngo Chek Ling, “An automated palmprint recognition system”, *Image and Vision Computing*, vol. 23, 2005, 501–515.

[20] T. UZ, G. Bebis, A. Erol and S. Prabhakar, “Minutiae- based template synthesis and matching for fingerprint authentication”, *Computer vision and Image Understanding*, vol. 113, 2009, 979-992.

[21] W. Jia, B.Ling, K-W. Cha and L. Heutte, “Palmprint identification using restricted fusion”, *Applied Mathematics and Computation* vol. 205, 2008, 927–934.

[22] W. Li, J. You, “Texture-based palmprint retrieval using a layered search scheme for personal identification”, *IEEE Trans. Multimedia*, vol. 7, n°5, 2005, 891–898.

[23] W. Li, L. Zhang, D. Zhang and J. Yan, “Principle line based ICP alignment for palmprint verification”, *ICIP 2009*, 1961-1964.

[24] X. Wang, B. Xian, J-F. Ma and X-L. Bi, "Scaling and rotation invariant analysis approach to object recognition based on Radon and Fourier–Mellin transforms", *Pattern Recognition*, vol. 40, 2007, 3503-3508.

[25] X.Wang, F.X Guo, B. Xiao and J-F. Ma, "Rotation analysis and orientation estimation method for texture classification based on Radon transform analysis", *J. Vis. Commun. Image*, vol. 21, 2010, 29-32.

[26] X. Wu, D. Zhang and K. Wang, "Fisherpalms based palmprint recognition", *Pattern Recognition. Letters*, vol. 24, 2003, 2829–2838.

[27] Y. W. Chen, Y.Q Chen, "Invariant descriptor and retrieval for planar shapes using Radon composite features", *IEEE transaction on signal processing*, vol. 56, n° 10, 2008, 4762-4771.